Available online at www.sciencedirect.com
ScienceDirect
Surface & Coatings Technology 201 (2006) 1962 – 1968
SURFACE & COATINGS TECHNOLOGY
www.elsevier.com/locate/surfcoat

Process and microstructure simulation in thermal spraying

Johannes Wilden *, Heiko Frank, Jean Pierre Bergmann

Ilmenau Technical University, Institute of Production Engineering, 98684 Ilmenau, Germany

Available online 18 July 2006

Abstract

Thermally sprayed coatings are widely used to improve wear and corrosion behavior of mechanical parts. To develop new coating processes and applications – a detailed knowledge of process–material interaction is necessary. According to the progress in computing and commercial software today simulation can be used to understand the interaction of process parameters with the material behavior like solidification, microstructure and residual stresses within the coating. Under commercial aspects the process parameters can be optimized to increase the deposition rate and minimize the residual stresses simultaneously. For plasma spraying the simulation of the coating process from plasma generation, particle injection, heating and acceleration to particle impact on the substrate, solidification and residual stresses and the influence of different parameters will be demonstrated and correlated to the experimental results.

Keywords: Process modelling; Vacuum plasma spray; Coating structure; Microstructure

1. Introduction

Thermally sprayed coatings are widely used to improve wear and corrosion behavior of mechanical parts. To develop new applications a detailed knowledge of process–material interaction and influence of process design on coating morphology and microstructure is necessary. The boundary conditions and the multitude of influencing parameters during the spray process make it nearly impossible to develop defined structures and morphologies only by experiments [1,2].

Thanks to the progress of computing and commercial software today simulation can be used to understand the interaction of process parameters with the material behavior like solidification, microstructure and residual stresses within the coating. The modeling of the spray process allows us to estimate the process conditions and coating microstructure with defined properties. Under commercial aspects costs of new coating systems can be reduced. Furthermore process parameters can be optimized in order to control the microstructure, to increase the deposition rate and to minimize the residual stresses simultaneously.

For vacuum plasma spraying the simulation of the coating process from plasma generation, particle injection, heating and acceleration, particle impact on the substrate, solidification and residual stresses and the influence of different parameters will be demonstrated and correlated to the experimental results. To use the model concept for different thermal spray processes only the heat generation, heat and momentum transfer has to be adapted to the regarded process.

2. Process modeling

2.1. Process description

In general thermal spray processes can be described by the following 5 steps: energy input, heating and acceleration, flattening on the substrate, nucleation and solidification, coating formation and determination of residual stresses (Fig. 1).

At first plasma generation and subsequent the heat and momentum transfer from the plasma onto the particles will be modeled. Depending on the heat and momentum transfer the particles will be partially or fully melted before their impact. Trajectories, velocity and temperature of the sprayed particles depend on plasma properties, injection conditions and feed stock material and size. On the substrate the particles will spread out and the resulting shape will depend on the particle temperature and velocity. In the next step nucleation and solidification of the particles occurs. The resulting microstructure depends on the

* Corresponding author. Tel.: +49 3677 69 2981; fax: +49 3677 69 1660.
E-mail address: johannes.wilden@tu-ilmenau.de (J. Wilden).

0257-8972/$ - see front matter © 2006 Elsevier B.V. All rights reserved.
doi:10.1016/j.surfcoat.2006.04.059

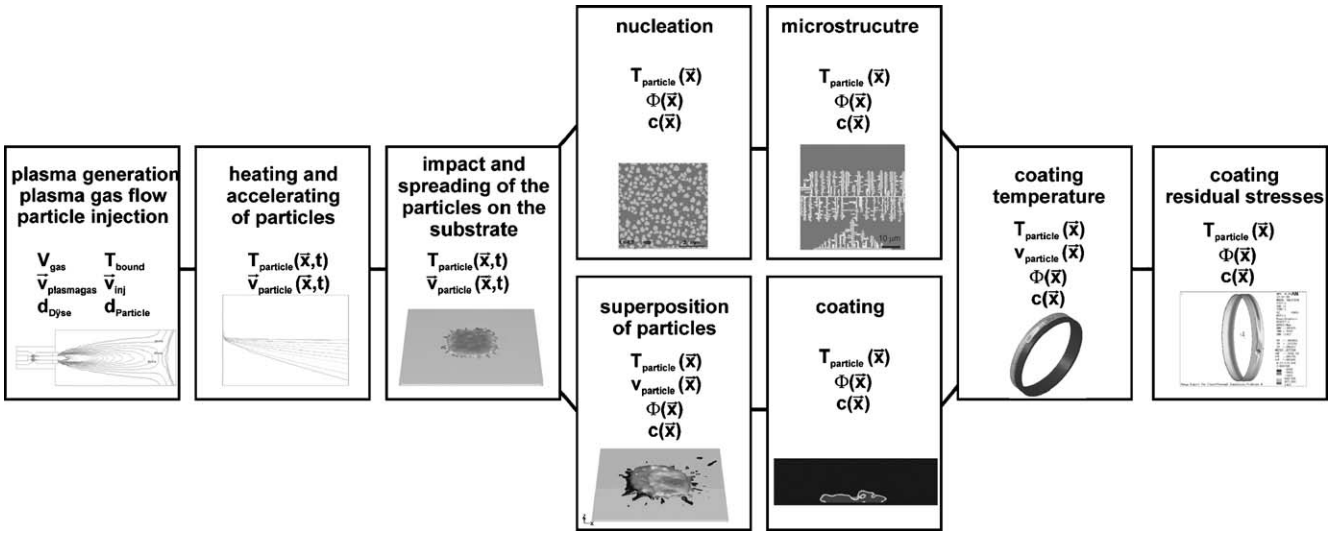

Fig. 1. Modeling of vacuum plasma spraying — modeling steps.

temperature gradient and cooling rate. The superposition of many particles leads to a complete coating with defined properties. Residual stresses within the coating are influenced by thermo-mechanical effects during heating and cooling of the coating.

The process steps are simulated successively with regard to the physical behavior (melting, solidification, turbulent flow, laminar flow) and the time scales.

2.2. Theoretical background

The simulation of plasma generation, plasma gas flow and plasma particle-interaction is based on the fluid dynamics of viscous liquids under consideration of energy input, melting and solidification processes. The flow of the plasma gas into the spray chamber is described by the fundamentals of the dynamic flow of a viscous fluid [3]. According to these basic relationships, the velocity field of the plasma can be determined by the Navier–Stokes Eq. (1) for the dynamical flow.

$$\rho\frac{\partial\bar{\vec{v}}}{\partial t}+\nabla\left(\rho\bar{\vec{v}}\cdot\bar{\vec{v}}\right)+\nabla\left(\overline{\rho\vec{v}'\vec{v}'}\right)=-\nabla\bar{p}+\eta\Delta\bar{\vec{v}}+\frac{1}{3}\eta\left(\nabla\left(\nabla\bar{\vec{v}}\right)\right)+\rho\vec{g}+\vec{F} \quad (1)$$

$\vec{F}$	External forces	$\vec{v}$	Plasma gas velocity	ρ	Density
$\vec{g}$	Gravitational Acceleration	p	Pressure	η	Dynamic Viscosity

Temperature and velocity distribution within the plasma jet can be calculated based on the description of the energy balance (Eq. (2)). The energy within the arc is calculated considering electrical power, heating, dissociation and ionisation of the plasma gas and energy loss by cooling. To calculate the energy transfer to the gas a simple channel shaped arc was assumed. A more detailed description of the dynamic behavior of the arc in the plasma spray torch can be found in [4].

$$\frac{\partial\vec{v}}{\partial t}\left[\rho\left(U+\frac{\vec{v}^2}{2}\right)\right]+\nabla\cdot\left[\rho\left(U+\frac{\vec{v}^2}{2}\right)\vec{v}\right]=\nabla\cdot(\lambda\nabla T)-\nabla(\vec{v}p)+\vec{v}(\eta\Delta\vec{v})+\frac{1}{3}\vec{v}\eta(\nabla(\nabla\vec{v}))+\rho\vec{g}\vec{v}+E_{\text{ext}}. \quad (2)$$

U	Internal energy	E_{ext}	External energy source

Additionally, the powder injection leads to a two-phase flow of discrete particles in the plasma. Particle trajectories can be calculated using the Lagrange equation of motion (Eq. (3)) under consideration of plasma gas flow and plasma particle interaction. The trajectories mainly depend on particle injection velocity v_{Part}, plasmagas density ρ_{gas} and particle mass and shape.

$$\frac{\partial\vec{v}_{\text{Part}}}{\partial t}=\vec{F}_{\text{Drag}}(\vec{v}_{\text{Gas}}-\vec{v}_{\text{Part}})+\left(\frac{\rho_{\text{Gas}}}{\rho_{\text{Part}}}\right)\vec{v}_{\text{Part}}\frac{\partial\vec{v}_{\text{Gas}}}{\partial\vec{r}}+\frac{1}{2}\frac{\rho_{\text{Gas}}}{\rho_{\text{Part}}}\frac{d}{dt}(\vec{v}_{\text{Gas}}-\vec{v}_{\text{Part}})+\vec{g}\left(\frac{\rho_{\text{Gas}}-\rho_{\text{Part}}}{\rho_{\text{Part}}}\right) \quad (3)$$

$\vec{F}_{\text{Drag}}$	Drag force

Table 1
Boundary conditions for calculation plasma generation and plasma–particle interaction

Parameter	Value	Parameter	Value
Chamber pressure	20.000 Pa	H_2 content of plasma gas	0…25%
Chamber temperature	300 K	Nozzle diameter	8 mm
Plasma power	25…50 kW	Particle material	Nickel
Plasma gas flow rate	30…70 slpm	Injection velocity	10…30 m/s
Plasma gas	Ar/H_2 mixture	Particle size	22…50 μm

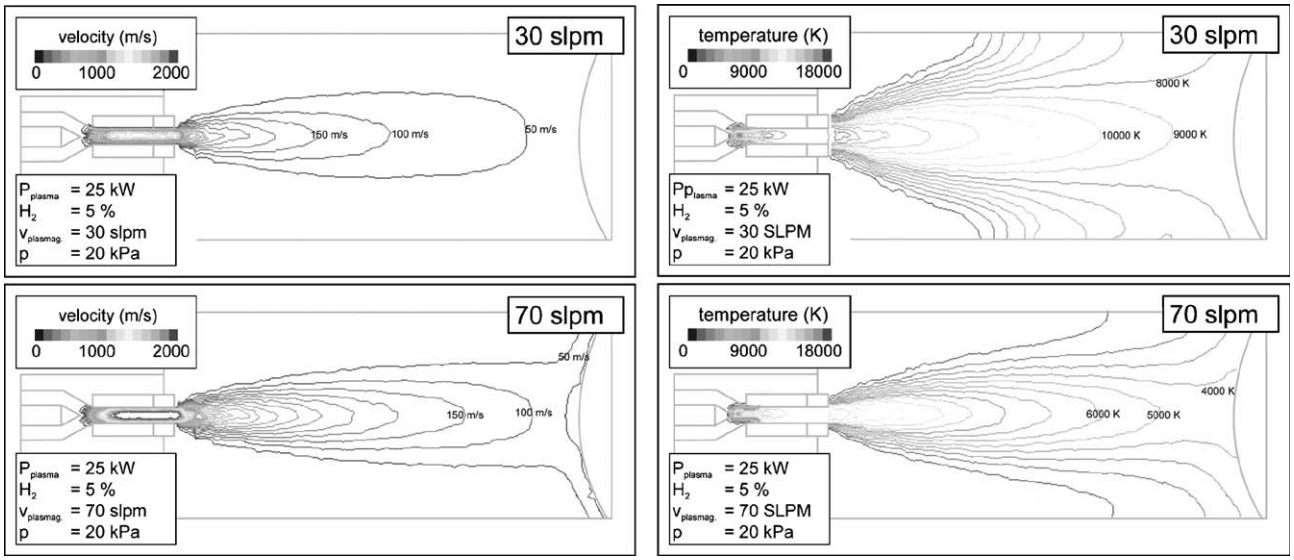

Fig. 2. Plasma gas velocity (left) and temperature (right) with different plasma gas flow rates.

The Volume Of Fluid (VOF) method can be used to describe the flattening of the particles (Eq. (4)) on the substrate regarding the state Φ of a cell.

$$\frac{\partial \Phi}{\partial t} + \vec{v} \cdot \nabla \Phi = 0 \tag{4}$$

The microstructure evolution of the coating depends on the nucleation and grain growth during solidification. Fundamentals of microstructure calculation are described by the phase field model for single-phase solidification. The state of the melt can be described by Φ. For $\Phi=1$ the area is liquid, $\Phi=0$ is defined as solid. The field function can be deduced from the Landau Ginzburg representation of the functional of the free energy.

$$F = \int_{\Omega} \left[f(\Phi, T) + \frac{1}{2} \in^2 (\nabla \Phi)^2 \right] d\Omega \tag{5}$$

Ω	Volume	$f(\Phi,T)$	Free energy density
$T(x,t)$	Temperature, depend on location and time	$\in$	Interface thickness

3. Plasma generation and plasma–particle interaction

Plasma temperature, plasma velocity and plasma–particle interaction are determined based on the boundary conditions and the process conditions (Table 1). The physical data for plasma gas temperature and velocity calculation are obtained from [5]. The material properties used are found in the literature [6].

As a first step, the influence of the plasma gas flow rate on the plasma jet velocity and the plasma temperature is determined. Calculations of plasma properties were done by setting the plasma gas flow rate between 30 and 70 slpm, the

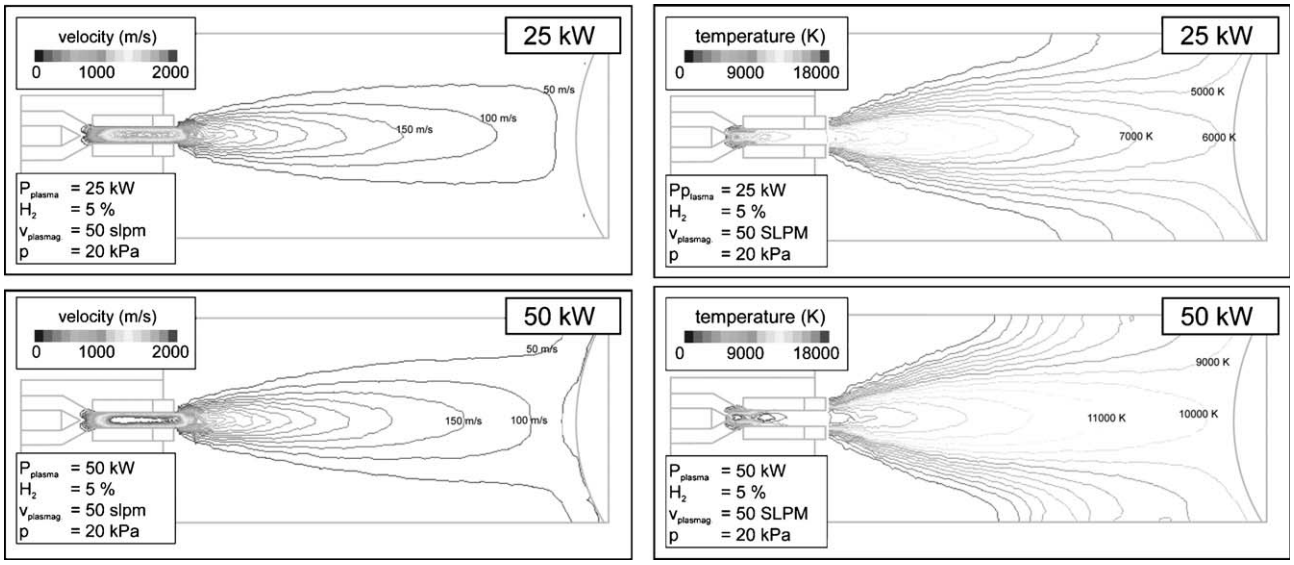

Fig. 3. Plasma gas velocity (left) and temperature (right) with different plasma power.

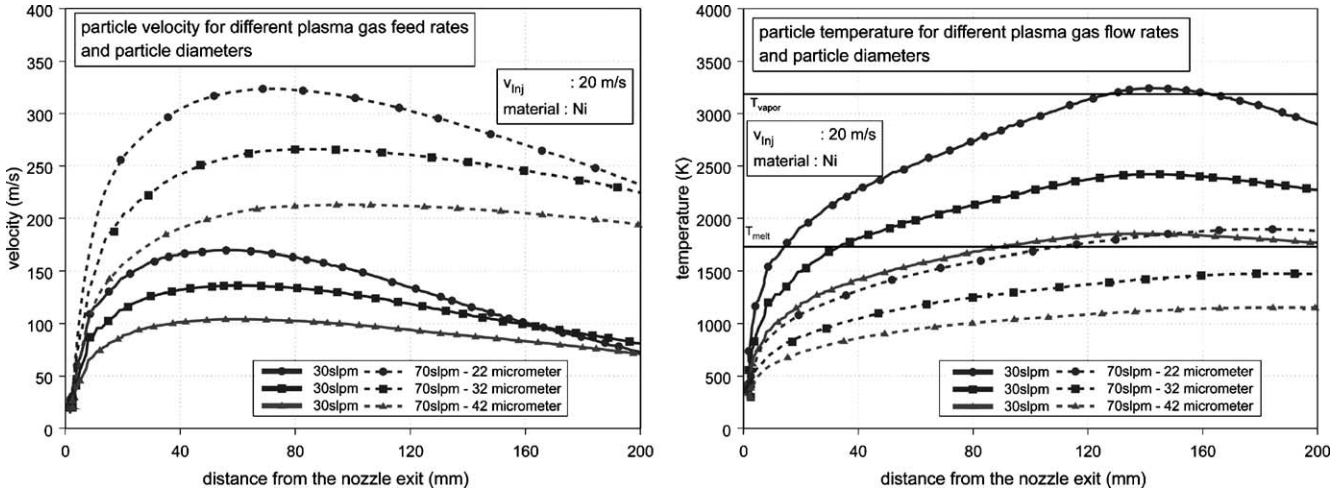

Fig. 4. Particle velocity and particle temperature for different gas flow rates.

hydrogen content between 0 and 25 at.-% H_2 and an arc power of 25 and 50 kW. In these investigations, the pressure of 20 000 Pa and the diameter of the nozzle of 8 mm were constant.

Fig. 2 shows the influence of the plasma gas flow rate on the plasma jet velocity and the plasma temperature. A higher flow rate leads to a higher velocity within the nozzle and the expanding plasma jet. An increased flow rate at constant arc power reduces the provided energy per volume. This results in a lower plasma temperature at a higher flow rate.

Differences in the energy input into the arc result in a low influence on the velocity of the gas jet, but a significant effect on the plasma gas temperature (Fig. 3). The electrical power was set at 25 and 50 kW, the plasma gas flow rate (50 slpm) and the hydrogen-concentration (5 at.-%) were constant. Doubling the power from 25 to 50 kW leads to an increase in the velocity within the nozzle and the expanding plasma jet (nozzle exit: velocity increases from 1644 to 1908 m/s). The higher power leads to a significant increase in the temperature within the nozzle due to the higher provided energy. At the nozzle exit, the temperature increases from 13,118 to 15,683 K with increasing power from 25 to 50 kW, near the substrate surface the temperature increases from 6012 to approximately 9916 K.

The particle temperature and velocity during variation of plasma gas flow rate and injection velocity depend on the distance from the nozzle exit and are shown in the next figures.

At a flow rate of 30 slpm, 200 mm down stream the nozzle exit the particle velocity is between 80 and 90 m/s. At a higher gas flow rate, the velocity increases up to 200 m/s (42 μm) and 230 m/s (22 μm) (Fig. 4). With increasing flow rate the temperature decreases due to the higher velocity of the particles and the resulting shorter dwell time in the plasma. Heating and melting smaller particles leads to higher particle temperatures. Higher plasma temperatures (in the case of 30 slpm) will lead to evaporation of small particles.

From Fig. 5 it can be concluded, that the variation of injection velocity only has a small influence on the particle velocity but a big effect on the particle temperature. The particle velocity is mainly dependent on the particle diameter. With increasing injection velocity particle temperature decreases due to the shorter dwell time in the plasma. In the case of higher particle diameters and higher injection

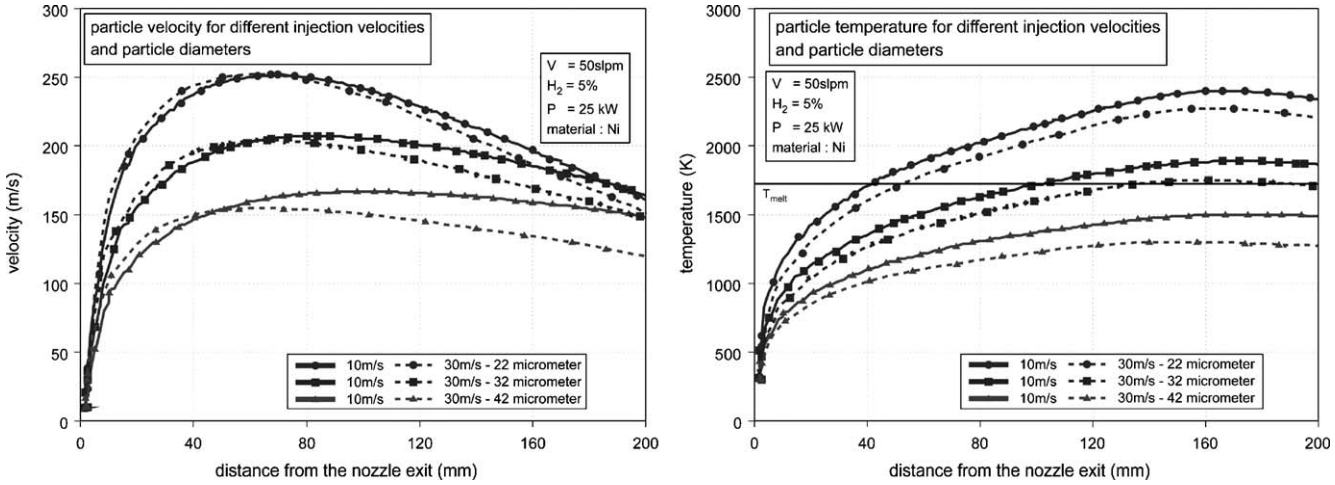

Fig. 5. Particle velocity and particle temperature for different injection velocities.

Table 2
Boundary conditions for calculation of particle spreading and coating formation

Parameter	Value	Parameter	Value
Particle temperature	1500...3000 K	Substrate temperature	300–1000 K
Particle velocity	30...200 m/s	Substrate thickness	0.1–5 mm
Particle size	22–50 μm	Substrate material	Ni, Fe, Cu
Particle material	Ni	Heat transfer coefficient	4000 W m^{-2} K^{-1}
		Emission coefficient	1×10^8 W m^{-3}

velocities, the particle temperature is lower than the melting temperature.

4. Particle spreading and coating formation

The spreading of the particles depends on the properties calculated in the previous simulation steps. Depending on plasma and particle properties and the process conditions, the shape of spreaded and overlayed particles varies. Particle spreading and coating formation were calculated based on the boundary conditions and the process parameters given in Table 2. The used material properties are found in literature [6].

Overlaying of several particles with different properties leads to a coating with a more complex shape. The energy input of every splashed particle changes the geometry and leads to additional heating and sometimes remelting of the predeposited particles in the coating and at least to an inhomogeneous shape with pores within the solidified material.

After splashing and overlaying of 12 particles processed by 50 kW, Plasma gas Ar (0 at .-% H_2) and a gas flow rate of 70 slpm (calculated particle temperature between 1461 and 2244 K, calculated particle velocity between 250 and 331 m/s) the geometry given in Fig. 6 is formed. The high kinetic energy induces a partially break up of the surface and a partial particle remelting. This leads to a ring like structure with a rough surface geometry with splashed secondary spots and fingers. The cross section (Fig. 6, right) shows the non uniform overlaying of the particles. Molten material flowing across solidified regions partially remelts them and form pores. The resulting geometry is characterized by large pores and an area with a surface break up.

In addition to the particle properties, the substrate properties (material, temperature, cooling, surface geometry) influence the coating structure. At reduced plasma gas flow rate the particle temperature is higher (1606–2460 K) and particle velocity is lower (191–275 m/s) compared to Fig. 6. At a constant substrate temperature of 300 K, the geometry after impact of 12 particles is changed significantly.

It can be seen in Fig. 7 that the resulting coating geometry is flatter. The constant substrate temperature allows a constant heat transfer to the substrate and a faster cooling of the particles during the whole process. Due to the constant heat transfer, remelting processes within the coating were reduced, the surface is more stable and molten particles flow uniformly across already spread particles. The resulting cross sections show a more homogeneous geometry with a uniform coating thickness and only a few pores (Fig. 7, right).

At reduced plasma gas flow rate of 50 slpm, the particle temperature is between 1606 and 2480 K, the impact velocity is reduced to values between 191 and 275 m/s. Spreading and overlaying of 12 particles leads to the surface geometry given in Fig. 8. The geometry shows splashed parts and fingers because of the additionally heat input of the particles. Also the high kinetic and thermal energy of particles leads to remelting within the coating but without a surface break up. The cross section after the impact of 12 particles shows pores near the substrate and within the coating as well as partially remelted areas with a low coating thickness.

5. Microstructure

Solidification starts at the moment of the impact of the particles on the substrate. The temperatures of the particles and the substrate as well as the interface temperature between particles have an effect on the nucleation and the resulting microstructure.

In simulation studies the influence of the interface temperature between two flattening particles was investigated. At low interface temperatures, the boundary between the particles can be set as solid. Heterogeneous nucleation occurs at the interface so that nuclei grow into the particles (Fig. 9, left). A higher interface temperature (a few degrees below the melting point) leads to remelting and re-solution of the

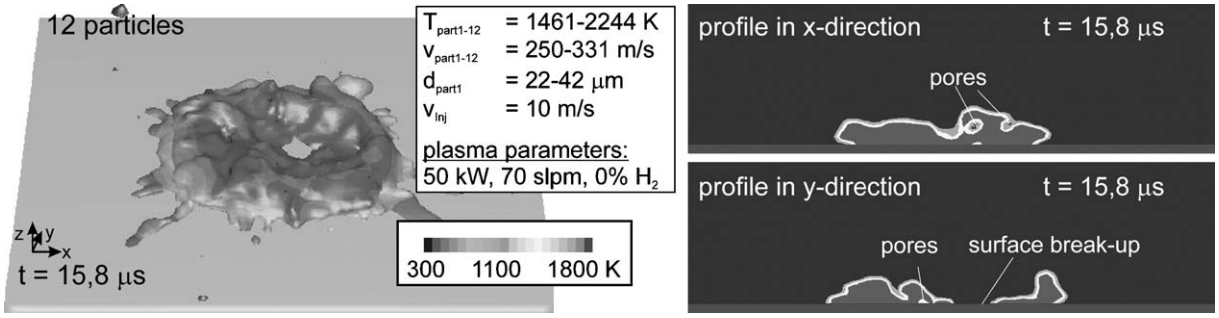

Fig. 6. Surface temperature and perpendicular cross sections after impact of 12 Ni-particles with different particle properties on a flat substrate without substrate cooling.

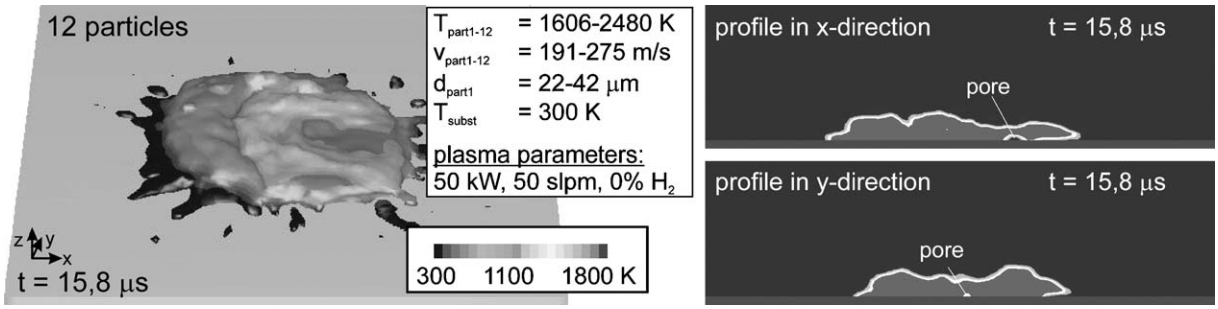

Fig. 7. Surface temperature and perpendicular cross sections after impact of 12 particles on a substrate at constant temperature of 300 K.

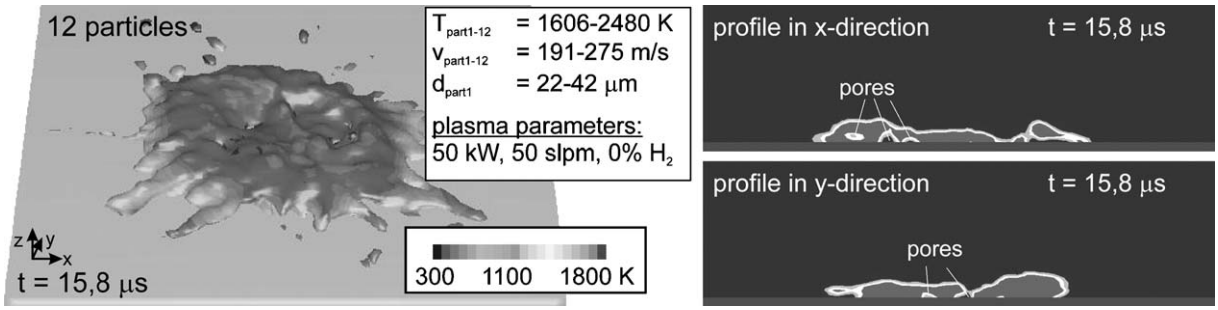

Fig. 8. Surface temperature and perpendicular cross sections after impact of 12 Ni-particles with different particle properties on a flat substrate without substrate cooling.

interface (Fig. 9, right) during solidification caused from the release of the latent heat. Dendrites can grow through the two particles. In both cases, the dendrite arm spacing is significantly influenced by the undercooling of the melt and the interface temperature.

6. Conclusion

In this paper, the results of developing a model for simulation of the thermal spray process were presented. The model includes the process steps plasma generation, plasma–particle interaction, coating formation, solidification and the determination of residual stresses. Investigations concerning the influence of the process parameters on plasma and particle properties show, that variations in electrical power, H_2-concentration and plasma gas flow rate have an effect on the temperature and the velocity of the particles before impact. These different particle properties influence the geometry of the deposited coatings. By variation of the substrate temperature and particle parameters (temperature, velocity, size) before the impact, coatings with an even shape and low porosity can be produced. Microstructure simulations have shown that for defined boundary conditions the dendrites grow through two and more splashed particles.

The results of the calculations have demonstrated that experimental investigations can partially be replaced by simulations. Adjusting defined process parameters for generating defined coating structures and for reducing residual stresses by simulations makes it easier to develop new coating systems with defined properties with less experimental effort.

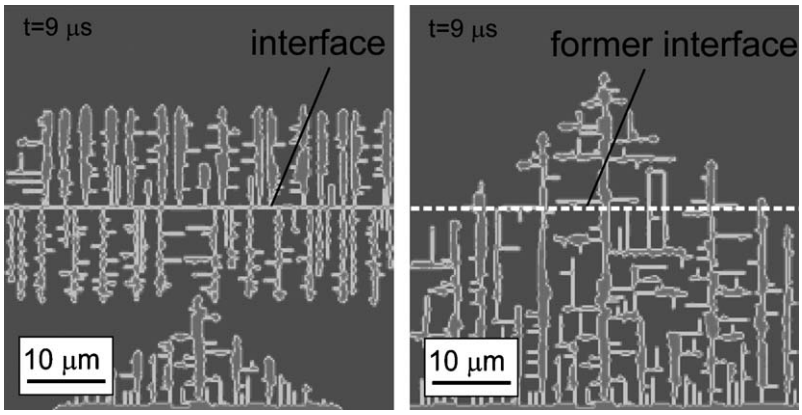

Fig. 9. Microstructure during solidification of two Ni particles with increasing interface-temperature.

References

[1] F. Kassabji, "Thermal Spray Application for the Next Millennium- A Business Development Perspective", Thermal Spray, Proceedings Thermal Spray Conference, Nice, 1998.
[2] J.R. Fincke, "A Computational Examination of the Sources of Statistical Variance in Particle Parameters During Thermal Plasma Spraying", Proceedings, ITSC 2000, Montreal, pp. 115-124.
[3] H. Oertel Jr., Prandtl-Führer durch die Strömungslehre, Vieweg and Sohn, Braunschweig/Wiesbaden, 2001.
[4] C. Baudry, A. Vardelle, Three-dimensional and time-dependent model of the dynamic behavior of the arc in a plasma spray torch; Proceedings of the ITSC 2004, Osaka, JP, ISBN: 3-87155-792-7, May 10–12 2004.
[5] M.B. Boulos, P. Fauchais, E. Pfender, Thermal Plasmas, Fundamentals and Applications, vol. 1, Plenum Press, New York, 1994.
[6] D'Ans, Lax, Taschenbuch für Chemiker und Physiker, Springer, 1998.